

# **Photodegradation of Atmospheric Chromophores: Changes in Oxidation State and Photochemical Reactivity**

Zhen Mu<sup>a</sup>, Qingcai Chen<sup>a\*</sup>, Lixin Zhang<sup>a</sup>, Dongjie Guan<sup>a</sup> and Hao Li<sup>a</sup>

<sup>a</sup> *School of Environmental Science and Engineering, Shaanxi University of Science and Technology, Xi'an 710021, China*

\*Corresponding authors:

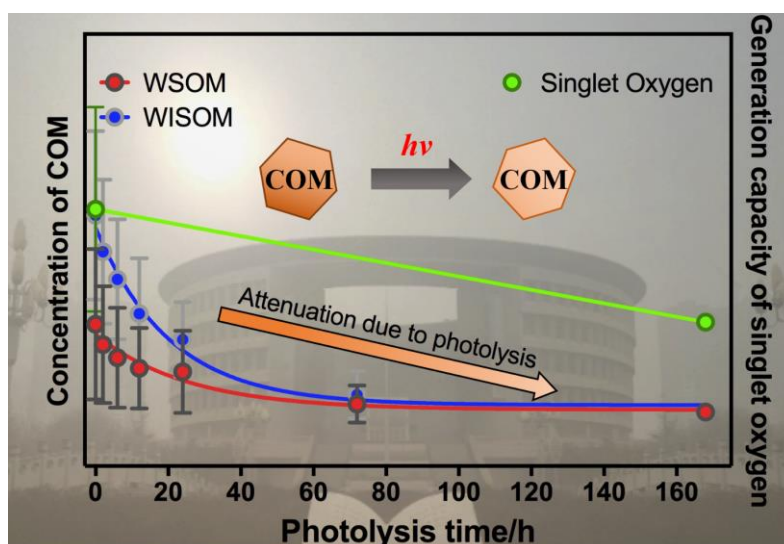
School of Environmental Science and Engineering, Shaanxi University of Science and Technology, Weiyang District, Xi'an, Shaanxi, 710021, China.

\*(Q. C.) Phone: (+86) 0029-86132765; e-mail: chenqingcai@sust.edu.cn;

1 **Abstract:** Atmospheric chromophoric organic matter (COM) can participate in photochemical  
2 reactions because of the photosensitivity, thus COM has a potential contribution to aerosols aging.  
3 However, the effect of COM photodegradation on photochemical reactivity and aerosol aging are  
4 not fully understood. Here, we report the potential impacts of photodegradation on carbonaceous  
5 components, optical properties, fluorophores components, and photochemical reactivity. We  
6 confirm that both water-soluble and water-insoluble COM are photodegraded, and fluorescent  
7 intensities decrease by 70% on average. Furthermore, low oxidation humic-like substance (HULIS)  
8 is converted into high oxidation HULIS, the result suggests that oxidation of HULIS can be used to  
9 trace the degree of aerosols aging. COM Photodegradation has a significant impact on  
10 photochemical reactivity. The content of triplet state COM decreases slightly in ambient particulate  
11 matter but increases in primary organic aerosol following photodegradation. The result highlight  
12 that photodegradation has opposite effect on different aerosols as a result of the changes in  
13 components. The ability of COM generating singlet oxygen declines obviously, which is consistent  
14 with optical properties. Photodegradation of precursors limit singlet oxygen generation and affect  
15 the aerosol photochemistry process. In conclusion, COM photodegradation not only change the  
16 compositions and properties, but also change aerosol aging.

17 **Key word:** atmospheric chromophores; photodegradation; EEMs; triplet state; reactive oxygen  
18 species.

19 **TOC:**



20  
21  
22  
23

## 24 **1. Introduction**

25 Atmospheric chromophoric organic matter (COM) mainly originate from biomass combustion  
26 emissions and secondary aerosols (Andreae & Gelencser, 2006; Budisulistiorini et al., 2017; Graber  
27 & Rudich, 2005; Zappoli et al., 1999). Because of the significant absorption for short-wave radiation  
28 (Wavelength range from near-ultraviolet light to visible light) (Rosario-Ortiz and Canonica, 2016;  
29 Cheng et al., 2016), COM may undergo photochemical process and have a significant impact on  
30 atmospheric components and quality (Zhao et al., 2013; Jo et al., 2016). Therefore, simulation and  
31 evaluation of COM photochemistry is necessary for understanding aerosol aging.

32 As photosensitive substances, the optical properties and components of COM change  
33 significantly under solar irradiation (Alkinson et al., 2016; Carlton et al., 2007; Lee et al., 2013;  
34 Murphy et al., 2013). On the one hand, optical properties change significantly due to chromophores  
35 are photo-bleached in aerosols. For example, Lee et al. (2014) reported that the mass absorption  
36 coefficients (MAE) of second organic aerosol (SOA) continue to decrease in the UV-Vis spectral;  
37 Zhong and Jang (2014) illustrated that MAC decreased by 41% on average because of the bleaching  
38 of wood-burning OM. The reason was the major components of wood-burning OM, such as  
39 conjugated aromatic rings and phenols, and hydroxyl groups, could be photodegraded. On the other  
40 hand, photodegradation has a significant effect on the composition of COM. Photodegradation can  
41 cause that COM decompose into small molecules and COM may have lower volatility and higher  
42 oxidation degree after photodegradation (Grieshop et al., 2009). COM could also be generated,  
43 which could be attributed to the formation of SOA during the photochemical reaction process. For  
44 example, Oligomeric COM could be generated by a mixture of anthracene and naphthalene  
45 suspensions through self-oxidation under solar irradiation and photo-oxidation of aromatic isoprene  
46 oxides are an important source of high-molecular-weight COM (Altieri et al., 2006; Altieri et al.,  
47 2008; Haynes et al., 2019; Holmes and Petrucci, 2006; Perri et al., 2009). Previous studies (Zhong  
48 & Jang, 2014; Saleh et al., 2013; Harrison et al., 2020) also have illustrated that SOA may have a  
49 more significant ability on light absorption than POA in the short-wavelength visible and near-UV  
50 region. As a result, photochemical process may play an important role in the components and  
51 properties of COM. Changes in chemical composition and optical properties also have a significant  
52 impact on photochemical activity in turn. There are limited studies that comprehensive exploring  
53 the components and properties transformation of COM in aerosols during the photodegradation  
54 processes.

55 Atmospheric COM could participate in the complex photochemical reaction, which further  
56 affect the aerosol aging (Mang et al., 2008). On the one hand, COM participates in atmospheric  
57 photochemical processes as a reactant. For example, COM can be oxidized by hydroxyl radicals  
58 ( $\bullet\text{OH}$ ) (Zhao et al., 2015) and the formation of polyols can be attributed to photooxidation of  
59 isoprene, which could be initiated by  $\bullet\text{OH}$  (Claeys et al., 2004). Humic-like substance (HULIS) with  
60 complex functional groups has significant contribution to photochemistry (George et al., 2015;  
61 Nebbioso & Piccolo, 2013; Wenk et al., 2013). On the other hand, COM participates in atmospheric

62 photochemistry process indirectly through generating reactive intermediates. Upon light absorption,  
63 high-energy singlet state COM ( $^1\text{COM}^*$ ) could be generated.  $^1\text{COM}^*$  deactivate quickly with the  
64 ways of emitting photon (fluorescence) and intersystem crossing (triplet state,  $^3\text{COM}^*$ ).  $^3\text{COM}^*$   
65 can generate reactive oxygen species (ROS), such as singlet oxygen ( $^1\text{O}_2$ ), super oxide ( $\bullet\text{O}_2^-$ ) and  
66  $\bullet\text{OH}$ , which indicate that  $^3\text{COM}^*$  play a critical role in ROS formation and pollutant attenuation  
67 (Paul Hansard et al., 2010; Szymczak & Waite, 1988; Zhang et al., 2014; Rosario-Ortiz and  
68 Canonica, 2016; Sharpless, 2012; Haag and Gassman, 1984; Zhou et al., 2019). A lot of DOM, such  
69 as aromatic ketones (Cannonica et al., 2006; Marciniak et al., 1993), benzophenone (Encinas et al.,  
70 1985), and phenanthrene (Wawzonek & Laitinen, 1942), have been identified as the precursor of  
71  $^3\text{COM}^*$ . Probes, such as 2,4,6-trimethylphenol (TMP) and sorbic acid (SA), are applicable to  
72 evaluate the chemical reactivity (Zhou et al., 2019; Moor et al., 2019; Chen et al., 2021). Why  
73  $^3\text{COM}^*$  is employed not  $^1\text{COM}^*$ ? The reasons are lower formation rate (15–100 times slower than  
74  $^1\text{COM}^*$ ), lower quenching rate (20000 times lower than  $^1\text{COM}^*$ ), and higher steady-state  
75 concentrations of  $^3\text{COM}^*$  (200~1300 times higher than  $^1\text{COM}^*$ ) (McNeil et al., 2016). Considering  
76 the potential effect of COM on aerosol aging and quality, it is necessary to clarify the path and  
77 mechanism.

78 COM photochemistry may dominate the chemical composition and aerosol aging. In order to  
79 illustrate the properties of COM photodegradation and the effect of COM photodegradation on  
80 aerosol aging, we simulate the process of COM photodegradation and COM generating ROS in  
81 laboratory. The objectives of the study are (1) to clarify the characteristics of carbonaceous  
82 components variation during COM photodegradation process, (2) to explore the effects of photo-  
83 degradation on the fluorophores and optical properties of water-soluble and water-insoluble  
84 chromophores, and (3) to investigate the effects of COM photodegradation on photochemical  
85 reactivity and aerosol aging (photochemical reactivity is characterized by triplet state and singlet  
86 oxygen generation capacity).

## 87 **2. Experimental Section**

### 88 *2.1 Sample Collection*

89 A total of 16 samples were collected (The details of the samples are shown in **Table S1** of SI).  
90 The ambient PM samples were collected in Shaanxi University of Science and Technology, Xi'an,  
91 Shaanxi Province (N34°22'35.07", E108°58'34.58"; the altitude of sampling location is about 30  
92 m). The ambient PM samples were collected on quartz fiber filter (Pall life sciences, Pall  
93 Corporation, America) by an intelligent large-flow sampler (Xintuo XT-1025, Shanghai, China)  
94 with a sampling time of 23 h 30 min and a sampling flow rate of 1000 L/min. The ambient PM  
95 samples were stored in the refrigerator at -20 °C prior to use.

96 The POA samples were collected through a combustion chamber. Straw and coal burning are  
97 the main way of heating and cooking in the rural areas in China. Therefore, wheat straw-, corn  
98 straw-, rice straw- and wood-burning samples were collected (Schematic diagrams of combustion

99 equipment is shown in **Figure S1**). The POA samples were stored in the refrigerator at -20 °C prior  
100 to use.

### 101 *2.2 Photodegradation experiment*

102 A quartz reactor was designed for photolysis experiment (Schematic diagrams of the  
103 photochemical devices are shown in **Figure S2**; The detail of the reactor has been described in  
104 previous study (Chen et al., 2021)). The illumination times were 0 h, 2 h, 6 h, 12 h, 24 h, 3 d and 7  
105 d, respectively. Two capsules (**Figure S2(b) & (c)**) were designed for triplet state and ROS  
106 generation experiment.

### 107 *2.3 Carbonaceous components analysis*

108 The original and photolyzed samples were ultrasonic extracted with ultrapure water (>18.2  
109 MΩ•cm, Master series, Hitech, China) and filtered through a 0.45 μm filter (Jinteng, China) to  
110 obtain the water-soluble organic matter (WSOM). After water extraction, the extracted filters were  
111 further extracted with methanol (HPLC Grade, Fisher Chemical, America) and filtered through a  
112 0.45 μm filter to obtain water-insoluble organic matter (WISOM). The blank samples were also  
113 extracted with the same method.

114 The analytical method of carbonaceous components has been described previously (Mu et al.,  
115 2019). Briefly, 100 μL extracts were injected on the baked quartz filter. Then, the wet filters were  
116 dried out by a rotary evaporator and the dried filters were analyzed by the OC/EC online analyzer  
117 (Model 4, Sunset, America) with the approach of NIOSH 870 protocol (Karanasiou et al., 2015).  
118 Six parallel samples were analyzed and the uncertainty of the method was <3.7% (one standard  
119 deviation).

### 120 *2.4 Optical analysis*

121 The light absorption and EEM spectra of the extracts were measured by an Aqualog  
122 fluorescence spectrophotometer (Horiba Scientific, America). The range of excitation wavelength  
123 was 200-600 nm and the range of emission wavelength was 250-800 nm. The interval was 5 nm.  
124 The exposure time was 0.5 s. The absorption spectra were also recorded in the wavelength range of  
125 200-600 nm. Water and methanol background samples were measured using the same method and  
126 the background signals were subtracted from the sample signals. The extracts were diluted to reduce  
127 internal filtration effect (The concentrations and dilution factors are shown in **Table S2** of SI).

128 The EEM data was analyzed by the PARAFAC model to identify fluorophores (The detailed  
129 analysis process refers to the previous papers, (Murphy et al., 2013; Chen et al., 2016a; Chen et al.,  
130 2016b)). WSOM and WISOM (111 samples) were combined in the dataset to create the PARAFAC  
131 model. According to the EEM characteristics and the residual error variation trend of the 2-7  
132 component PARAFAC models, 4 component PARAFAC model was selected (Analysis error of the  
133 models are shown in **Figure S4** of SI).

### 134 *2.5 Triplet state generation experiment*

135 As short-lived reactive intermediates, <sup>3</sup>COM\* have an important impact on photochemical  
136 process in atmospheric environment (Kaur et al., 2018). Therefore, changes in <sup>3</sup>COM\* generation

137 ability before and after photodegradation were studied. Chemical probe 2,4,6-trimethylphenol  
138 (TMP) was used as the capturing agent for the triplet state. 60  $\mu\text{L}$  of WSOM extracts (WSOC  
139 concentrations are shown in **Table S3**) and 60  $\mu\text{L}$  of TMP solution ( $c_{\text{TMP}} = 20 \mu\text{M}$ , Aladdin, China)  
140 were mixed in the capsule (**Figure S2(b)**). The capsule was placed in the reactor (**Figure S2(a)**).  
141 The illumination times was 0, 5, 10, 15, 30, 45, 60 and 90 min, respectively. Then 90  $\mu\text{L}$  mixed  
142 solution was taken out from the capsule at different time points and 30  $\mu\text{L}$  of phenol solution ( $c_{\text{phenol}}$   
143 = 50  $\mu\text{M}$ , Aladdin, China) were added into the mixed solution (Phenol solution was used as the  
144 internal standard substance for TMP quantification).

145 TMP was quantified by liquid chromatography (LC). The method of LC are as follows: C18  
146 column (Xuanmei, China); mobile phase: acetonitrile/water = 1/1 (v/v); flow rate: 1 mL/min; UV  
147 detector: detection wavelength 210 nm. The retention time is 14.5 min. Kaur & Anastasio (2018)  
148 and Richards-Henderson et al. (2015) have reported that TMP consumption conform to first-order  
149 kinetics. The first-order kinetic equation was used to fit exponential relationship among the TMP  
150 concentration ( $c_{\text{TMP}}/\mu\text{M}$ ), the illumination time ( $t/\text{min}$ ) and triplet state generation rate constants  
151 ( $k_{\text{TMP}}/\text{min}^{-1}$ ):

$$152 \quad c_{\text{TMP}} = a \cdot e^{-t \times k_{\text{TMP}}} \quad (1)$$

### 153 2.6 Singlet oxygen generation experiment

154 The effects of the COM photodegradation on singlet oxygen were studied. 4-Hydroxy-2, 2, 6,  
155 6-tetramethylpiperidine (TEMP,  $c_{\text{TEMP}}=240 \text{ mM}$ , Aladdin, China) was used as the capturing agent  
156 for singlet oxygen and captured singlet oxygen was quantified by EPR spectrometer (MS5000,  
157 Freiberg, Germany). Sorbic acid (SA,  $C_{\text{SA}}=133.3 \mu\text{M}$ , Aladdin, China) was used as quenching agent  
158 for triplet state. The method was as follows: (1) 40  $\mu\text{L}$  WSOM, 40  $\mu\text{L}$  TEMP and 40  $\mu\text{L}$  ultra-pure  
159 water were mixed in the capsule (**Figure S2(c)**). Then, 50  $\mu\text{L}$  of the mixed solution was taken out  
160 by capillary for EPR analysis; (2) 40  $\mu\text{L}$  WSOM, 40  $\mu\text{L}$  TEMP and 40  $\mu\text{L}$  ultra-pure water were  
161 mixed. The capsule was placed in the reactor for 60 min without illumination. Then 50  $\mu\text{L}$  mixed  
162 solution was taken out by capillary for EPR analysis; (3) 40  $\mu\text{L}$  WSOM, 40  $\mu\text{L}$  TEMP and 40  $\mu\text{L}$   
163 ultra-pure water were mixed. The capsule was illuminated in the reactor for 60 min. 50  $\mu\text{L}$  mixed  
164 solution was taken out by capillary for EPR analysis; (4) 40  $\mu\text{L}$  WSOM, 40  $\mu\text{L}$  TEMP and 40  $\mu\text{L}$   
165 SA solution were mixed. The capsule was illuminated in the reactor for 60 min, then 50  $\mu\text{L}$  mixed  
166 solution was taken out by capillary for EPR analysis.

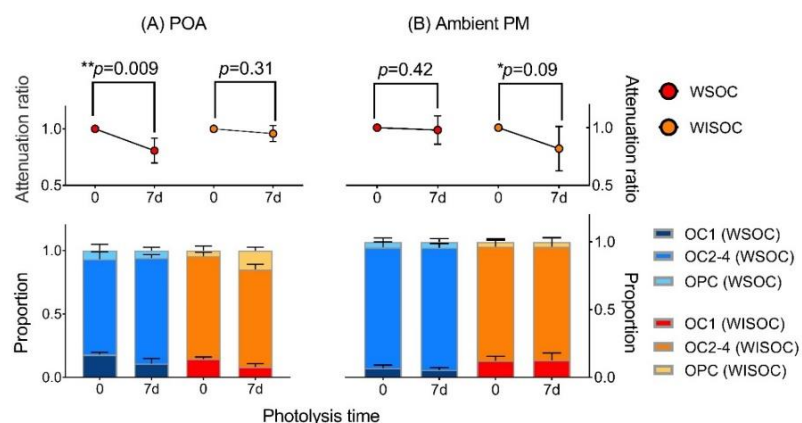
## 167 3. Results and discussion

### 168 3.1 Effect of COM photodegradation on carbonaceous components

169 COM can be decomposed and transformed in aerosol due to photodegradation (Wong et al.,  
170 2015). **Fig.1** describes the changes in the content of carbonaceous components before and after  
171 COM photodegradation. In POA, water soluble and water insoluble organic carbon (WSOC and  
172 WISOC) decrease by 22.1% and 3.5%, respectively. The results suggest that WSOC tend to be  
173 photodegraded in POA. As shown in **Fig.1(A)**, the proportion of OC1 in WSOC (OC1 and OC2-4

174 are the different stage in the process of thermal-optical analysis) decreases significantly, which is  
 175 the main loss of OC. OC1 are characterized by small molecular weight and highly volatile  
 176 (Karanasiou et al., 2015). The result suggests that OC with small molecular weight and highly  
 177 volatile tend to be photodegraded. In WISOC, there is a process of OC1 translating into pyrolysis  
 178 carbon (OPC). OPC in WISOM show an increasing trend (an average increase of 2.4 times). The  
 179 pyrolysis carbon is oxygen-containing substance. Thus, the increasing oxygen-containing organic  
 180 matter may be due to the photo-inducing oxidation reaction.

181 POA is fresh and ambient PM have undergone aerosol aging. In ambient PM (**Fig.1B**), WSOC  
 182 is nearly unchanged and WISOC decreases by 18.2%, which is opposite to POA. The results reflect  
 183 that WSOC has been photodegraded completely following the photodegradation and mineralization  
 184 process in ambient PM. However, WISOC with high molecular weight could not be photodegraded  
 185 completely and continue to be photodegraded in laboratory. The proportions of OC1, OC2-4, and  
 186 OPC are relatively stable in ambient PM, which indicate that the decreasing proportion in the  
 187 different stage are similar and the tendency is also opposite to POA. The result reflects that different  
 188 carbonaceous components have the similar abilities of photodegradation in ambient PM. Organic  
 189 matter with high molecular weight is photocomposed to small molecular weight and the molecular  
 190 weight tend to be consistent following the photodegradation.



191  
 192 **Fig.1** Changes in carbonaceous components before and after photodegradation. The  $p$ -value is the probability that  
 193 two sets of data have the same level (two-tailed test). \* and \*\* are represent the significant difference at the 0.1 and  
 194 0.01 levels, respectively.

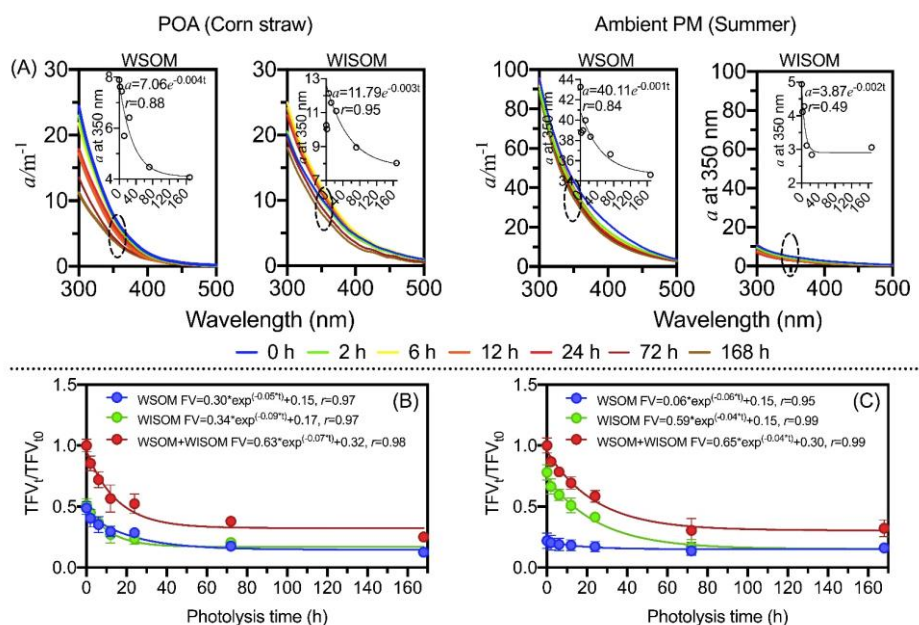
### 195 3.2 Effect of COM photodegradation on optical properties

196 As shown in **Fig.2**, both absorption coefficients and total fluorescence volume (TFV, RU-  
 197 nm<sup>2</sup>/m<sup>3</sup>) significantly decrease following aerosol photodegradation, which suggest that COM are  
 198 photo-bleached (Aiona et al., 2018; Duarte et al., 2005; Liu et al., 2016). The attenuations of  
 199 fluorescence and absorption coefficients are fit to first-order decay. The absorption coefficients  
 200 decrease by 32.0% and TFV decreases by 71.4% on average. However, as shown in **Fig.3**,

201 fluorescence intensities increase and decrease in different regions of EEMs (Aiona et al., 2018;  
 202 Timko et al., 2015).

203 In POA (**Fig.2(B)**), TFV decreases by 74.8% on average and the attenuation are fitted with  
 204 first-order decay kinetics. The attenuations of TFV are significant similarities between WSOM and  
 205 WISOM. Significantly, compared with most POA samples, the fluorescence intensity of wood-  
 206 burning COM only decreases by 9.0% (**Figure S7**), which is due to TFV of WISOM remain almost  
 207 unchanged. Secondary water-insoluble organic substances may be generated slightly in wood-  
 208 burning COM (Zhong & Jang, 2014). Changes in fluorescence intensities may also depend on the  
 209 types and water-insoluble wood-burning COM are difficultly photodegraded. In addition,  
 210 fluorophores photodegradation depend on the photochemical environment, such as solution pH  
 211 (Aiona et al., 2018), salinity (Xu et al., 2020), and temperature (Yang et al., 2021).

212 In ambient PM (**Fig.2(C)**), the decay rate constant of TFV in ambient PM ( $k = 0.04 \text{ h}^{-1}$ ) is  
 213 lower than in POA ( $k = 0.07 \text{ h}^{-1}$ ). TFV of water-soluble fluorophores decreases by 79.4% but water-  
 214 soluble fluorophores decreases by 26.7%. The attenuation of TFV and carbonaceous components  
 215 are identical with each other. The results suggest that water-insoluble fluorophores have greater  
 216 ability to be photodegraded than water-soluble fluorophores in ambient PM. It is worth noting that  
 217 72 h could be consider as the end point of aerosol aging because TFV maintain a constant value  
 218 after 72 h in POA and ambient PM.



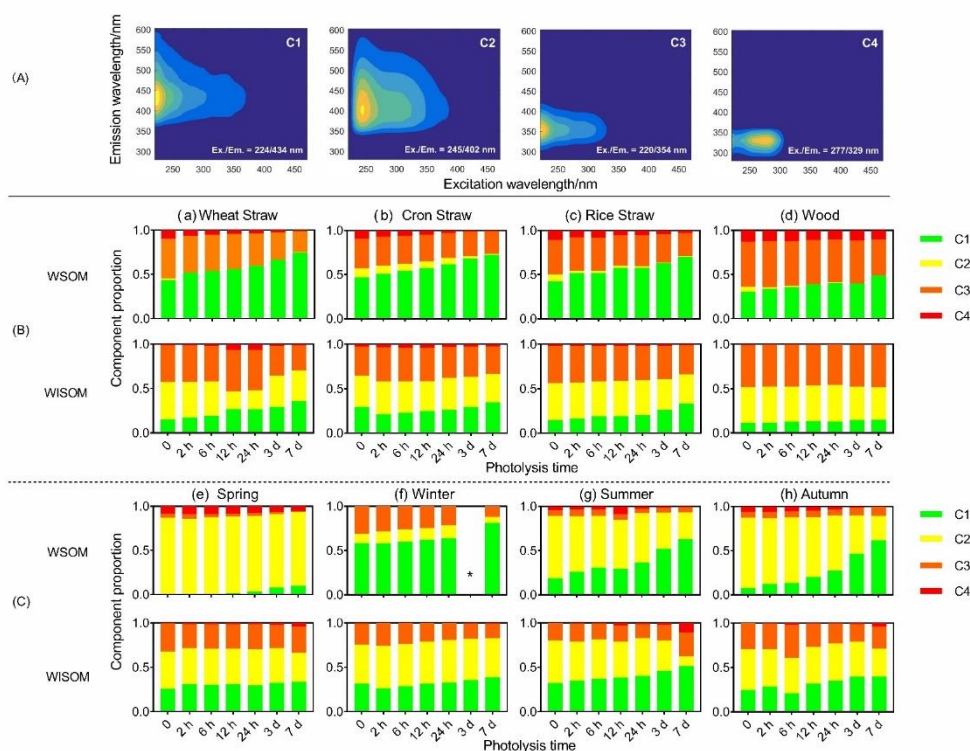
219  
 220 **Fig.2** Changes in light absorption and fluorescence volume during the photodegradation process. (A) Absorption  
 221 coefficient. The scatter plot is absorption coefficient at 350 nm. (B) and (C) the attenuation curve of fluorescence  
 222 volume in POA (except for the wood sample) and ambient PM, respectively.



223 Fluorophores compositions are studied by the approach of EEMs-PARAFAC (**Fig.3A**).  
224 Although previous study analyzed the water-soluble and water-insoluble fluorophores separately  
225 (Tang et al., 2020a), based on the Chen's studies (2020; 2016b), water-soluble and water-insoluble  
226 samples were combined to create the PARAFAC model to illustrate the distribution of fluorophores  
227 in WSOM and WISOM and solvent had no significant effect on the EEMs of complex mixtures in  
228 aerosols. Four fluorophores are identified. Four fluorophores are identified. The fluorescence peaks  
229 of C1 and C2 appear at (Ex./Em. = 224/434 nm) and (Ex./Em. = 245/402 nm). The peaks are similar  
230 to high and low oxidation humic-like substance (HULIS), respectively (Chen et al., 2016b; Birdwell  
231 and Engel, 2010). The peaks of C3 and C4 appear at (Ex./Em. = 220/354 nm) and (Ex./Em. =  
232 277/329 nm) and these two fluorophores are associated with protein-like organic matter (PLOM-1  
233 and PLOM-2) (Sierra et al., 2005; Huguet et al., 2009; Chen et al., 2016a and 2016b; Coble, 2007;  
234 Fellman et al., 2009).

235 The content of fluorophores changes significantly during the photodegradation process. In  
236 POA (**Fig.3B**), the content of high-oxidation HULIS (C1) increases significantly in WSOM and the  
237 relative content increases by 25.7% on average. Low oxidation HULIS (C2) and PLOM (C3&C4)  
238 decrease by 6.0% and 19.7%, respectively. Changes in proportion indicates that high-oxidation  
239 HULIS fluorophores (C1) could be generated and low oxidation HULIS(C2) and PLOM (C3&C4)  
240 may be photolyzed, which suggest that low oxidation HULIS (C2) could be converted into high  
241 oxidation HULIS (C1) due to photooxidation (Tang et al., 2020b; Chen et al., 2020). Furthermore,  
242 the content of high-oxidation HULIS (C1) also increases (average 17.5%) in WISOM, which can  
243 be attributed to photo-mediated secondary reaction.

244 In ambient PM (**Fig.3C**), the content of PLOM (C3&C4) in ambient PM (43.3%) is  
245 significantly lower than that in POA (19.4%). The content of high-oxidation HULIS increases and  
246 the low-oxidation HULIS decreases, which are similar to POA. Thus, high-oxidation HULIS could  
247 be used to trace the degree of aerosols aging.



248

249

250

251

**Fig.3** (A) EEM spectra of fluorophores; (B) Changes in proportion of fluorophores in POA; (C) Changes in proportion of fluorophores in ambient PM. \*: The data of 3-day photolysis of water-soluble chromophores in winter is unavailable.

252

### 3.3 Effect of COM photodegradation on aerosol photochemical reactivity

253

254

255

256

257

258

259

260

261

262

263

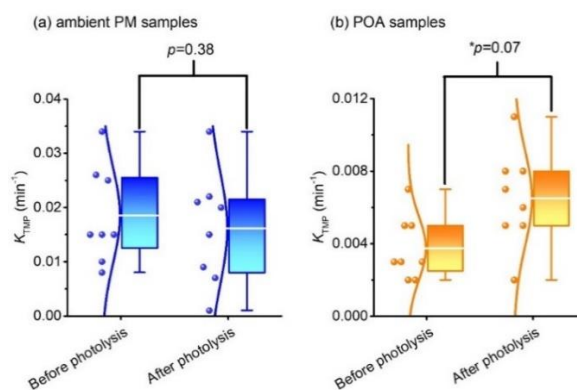
264

265

266

267

COM photodegradation has a significant effect on aerosol photochemical reactivity. The photochemical activity is characterized by the yield of  $^3\text{COM}^*$  and  $^1\text{O}_2$ . **Fig.4** show the difference of triplet state generation before and after the photodegradation (Details are shown in **Figure S8**). In ambient PM, the generation rate of triplet state decreases by 11% on average after COM photodegradation, while statistical analysis shows that the changes of triplet state generation are not obvious ( $p = 0.38$ , two-tailed test). On the contrary, photodegradation promote triplet state generation significantly, the triplet state generation rate increases by 75% on average in POA ( $p = 0.07$ , two-tailed test). Triplet state generation remains unchanged or increases following photodegradation. The results are unexpected and can be explained by recent study (Chen et al. 2021): On the one hand, only a small proportion of COM could generate triplet state in aerosols and Fluorophores does not represent the COM with the ability to generate triplet state. Therefore, triplet state generation could not be evaluated by fluorescence intensity. On the other hand, we use a high concentration of TMP, in this case, TMP mainly capture high-energy triplet state (Rosado-Lausell et al., 2013; Chen et al., 2021). Thus, COM, that could generate a high-energy triplet state, may not be photodegraded.



268  
269  
270  
271  
272

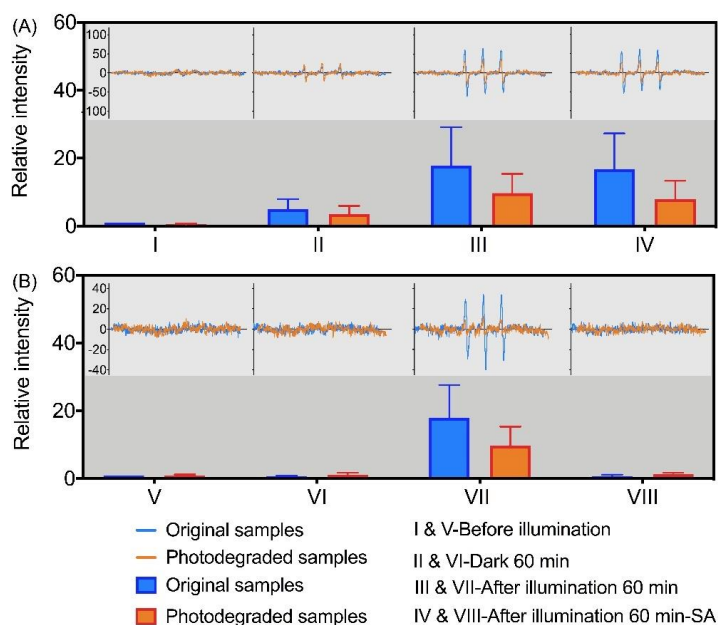
**Fig.4** Changes in the triplet state generation. (a) Ambient PM; (b) POA. The line from bottom to top in the box plots are minimum, first quartile, the average value (white lines), third quartile, and maximum, respectively. The  $p$ -value is the probability that two sets of data have the same level (two-tailed test). \* represents a significant difference at the 0.1 level.

273 COM can generate triplet state and further generate singlet oxygen (McNeill and Canonica,  
274 2016). The effect of COM photodegradation on singlet oxygen is studied. Typical EPR spectra of  
275  $^1\text{O}_2$  are shown in **Fig.5** (EPR spectra of all samples are shown in **Figure S9** and **Figure S10**). In the  
276 original POA samples (i.e., the original samples with photodegradation time of 0, the photodegraded  
277 samples with photodegradation time of 7d; details of samples are described in section 2.2),

278 In POA, (I) there is little  $^1\text{O}_2$  before illumination both in original and photodegraded samples;  
279 (II)  $^1\text{O}_2$  are generated both in original and photodegraded samples after 60 min in dark and the  
280 content of  $^1\text{O}_2$  in original samples is higher than that in photodegraded samples, which suggest POA  
281 could generate  $^1\text{O}_2$  without illumination; (III) As expected, compared with the samples without  
282 illumination, the content of  $^1\text{O}_2$  increases by 3 times both in original and photodegraded samples;  
283 after 60 minutes of illumination. Consistent with (II), the content of  $^1\text{O}_2$  in original samples is also  
284 higher than that in photodegraded samples (42.1%), which prove the inhibiting effect of COM  
285 photodegradation on  $^1\text{O}_2$ ; (IV) However, the content of  $^1\text{O}_2$  is not reduced when the triplet state is  
286 quenched by sorbic acid. Sorbic acid is a capturing agent for high-energy triplet state (triplet  
287 energies  $E_T = 239\text{-}247$  kJ/mol) (Zhou et al., 2019; Moor et al., 2019). Therefore, the results indicate  
288 that the low-energy  $^3\text{COM}^*$  ( $E_T < 239$  kJ/mol) may be the main precursor for  $^1\text{O}_2$  ( $E_T = 94$  kJ/mol)  
289 in POA.

290 In ambient PM, (V) the content of  $^1\text{O}_2$  in original and photodegraded samples is similar to POA;  
291 (VI) Compared with (V), the content of  $^1\text{O}_2$  almost unchanged after 60 min in dark, which is  
292 opposite to POA. The result suggests ambient PM could not generate  $^1\text{O}_2$  without illumination. (VII)  
293 The content of  $^1\text{O}_2$  increases significantly after 60 minutes of illumination and the content of  $^1\text{O}_2$  in  
294 original samples is higher than that in photodegraded samples (41.0%). (VIII) When the triplet state  
295 is quenched by sorbic acid, the signal of  $^1\text{O}_2$  disappears. The result suggests that  $^1\text{O}_2$  is mainly  
296 generated by high-energy  $^3\text{COM}^*$  in ambient PM. The above results show that the precursor of  
297 high-energy triplet state could be photodegraded, which directly lead to the decrease in  $^1\text{O}_2$  in  
298 ambient PM. In summary, a decrease in the yield of  $^1\text{O}_2$  because the inhibiting effect of COM

299 photodegradation on photochemical activity in ambient PM and POA and COM photodegradation  
 300 do not change the mechanism of low-energy  $^3\text{COM}^*$  generating  $^1\text{O}_2$  in POA. However, the  
 301 quenching effects of sorbic acid in POA and ambient PM are different because of the difference in  
 302  $^3\text{COM}^*$  energy.



303  
 304 **Fig.5** Changes in DOM generating  $^1\text{O}_2$  before and after photodegradation. (A) POA; (B) Ambient POA.

#### 305 **4. Implication**

306 We made a comprehensive study in COM photo-degradation and the effect of COM photo-  
 307 degradation on optical properties, chemical compositions, and photochemical activity. The  
 308 characteristics of COM photo-degradation were revealed. COM photodegradation could result in  
 309 reduction of carbonaceous components, attenuation of optical properties, and changes in  
 310 components. We also propose that the COM photodegradation should be evaluated from the three  
 311 aspects for further study. (1) The impact of COM photodegradation on carbonaceous content are  
 312 unclear. Previous studies have revealed that WSOC did not significantly change in the river DOM  
 313 (Gonsior et al., 2009) and 0.2% of DOC was mineralized (Tranvik et al., 1998). However, the  
 314 observation in the study suggests that changes in carbonaceous component is different in aerosols,  
 315 which could be attributed to the differences in original components. (2) Decreasing in optical  
 316 properties is significant. Absorption coefficient and fluorescence intensity can be thought of as a  
 317 tracer for molecular weight (Stewart & Wetzel, 1980). Therefore, optical properties could indicate  
 318 the changes in molecular weight of COM during the photodegradation process. The characteristic  
 319 could be suitable for exploring the impact of photodegradation on COM components. (3)  
 320 Photodegradation of COM may dominant the fluorophores components (Aiona et al., 2018; Timko  
 321 et al., 2015). High-molecular-weight COM could be decomposed into low-molecular-weight COM  
 322 during photodegradation process. The conversion of low-oxidation HULIS to high-oxidation  
 323 HULIS is observed. Changes in COM may represent the degree of organic substances oxidation.

324 Therefore, we suggested that optical parameter and degree of oxidation of organic molecules should  
325 be use for characterizing the aerosol photo-aging process (Maizel et al., 2017).

326 Photodegradation can not only change the properties and components of COM, but also change  
327 their photochemical activity, which furtherly has a potential impact on the aerosol fate.  
328 Photodegradation and/or conversion of COM could be considered to be the main influence factor  
329 for photochemical reaction capacity (McNight et al., 2001; Zepp et al., 1985). Photochemical  
330 activity was quantified by the yield of triplet state and  $^1\text{O}_2$ . However, two different methods, two  
331 different results. COM photodegradation can restrain  $^1\text{O}_2$  generation but the effect of  
332 photodegradation on  $^3\text{COM}^*$  are unclear. Photodegradation has a significant inhibiting effect on the  
333  $^1\text{O}_2$  yield in aerosols (Latch et al. 2006; Chen et al., 2018). We insist that aerosol aging would be  
334 changed by photodegradation due to the yield of  $^1\text{O}_2$  is changed. Changes in triplet state generation  
335 are uncertain in ambient PM and POA. There are two reasons for it. On the one hand, only a small  
336 amount of COM are the precursor of  $^3\text{COM}^*$  in aerosols. On the other hand, the energy of capturing  
337 agents was closely related to  $^3\text{COM}^*$  quantification and  $^3\text{COM}^*$  could not be captured completely.  
338 Other capturing agents may lead to different results. Thus,  $^3\text{COM}^*$  could not properly illustrate  
339 photo-degradation. COM photodegradation would be play an important role in the content of ROS  
340 and ROS could celebrate the COM photooxidation (Claeys et al., 2004). Given the results, the  
341 interaction effect is significant in aerosol.

342 In summary, atmospheric photochemistry process has a remarkable impact on aerosol aging.  
343 Prediction of atmospheric lifetime and improvement of quality are strongly associated with  
344 photochemistry. We prove that carbonaceous content, absorption coefficients, fluorescence  
345 intensity, and photochemical activities are useful to reflect COM photodegradation process and  
346 aerosol fate. In addition, COM photodegradation have different impact on chemical activity in  
347 different aerosols, which may have different mechanisms. Therefore, the mechanisms of COM  
348 photodegradation effecting aerosol photo-aging deserve further investigation.

349 **Data availability.** All data that support the findings of this study are available in this article and its  
350 Supplement or from the corresponding author on request.

351 **Supporting information.** Additional details, including Tables S1–S5, Figures S1–S10, calculation  
352 of optical characteristics of WSOM/WISOM, are contained in the SI.

353 **Author contributions.** QC and ZM designed the experiments and data analysis. ZM and LZ  
354 performed sample collection. ZM performed the photochemical experiment. ZM and DG performed  
355 the OC/EC analysis and optical analysis. HL performed the EPR analysis. QC prepared the paper  
356 with the contributions from all co-authors.

357 **Competing interests.** The authors declare that they have no conflict of interest.

358 **Acknowledgments.** We thank the National Natural Resources Foundation for its financial support.

359 **Financial support.** This work was supported by the National Natural Science Foundation of China  
360 (grant numbers 41877354 and 41703102).

## 361 **References**

- 362 Aiona, P. K., Luek, J. L., Timko, S. A., Powers, L. C., Gonsior, M., and Nizkorodov, S. A.: Effect of Photolysis on  
363 Absorption and Fluorescence Spectra of Light-Absorbing Secondary Organic Aerosols, *ACS Earth Space*  
364 *Chem.*, 2, 235-245, 10.1021/acsearthspacechem.7b00153, 2018.
- 365 Altieri, K. E., Carlton, A. G., Lim, H. J., Turpin, B. J., and Seitzinger, S. P.: Evidence for oligomer formation in  
366 clouds: Reactions of isoprene oxidation products, *Environ. Sci. Technol.*, 40, 4956-4960,  
367 <http://dx.doi.org/10.1021/es052170n>, 2006.
- 368 Altieri, K. E., Seitzinger, S. P., Carlton, A. G., Turpin, B. J., Klein, G. C., and Marshall, A. G.: Oligomers formed  
369 through in-cloud methylglyoxal reactions: Chemical composition, properties, and mechanisms investigated by  
370 ultra-high resolution FT-ICR mass spectrometry, *Atmos. Environ.*, 42, 1476-1490,  
371 <http://dx.doi.org/10.1016/j.atmosenv.2007.11.015>, 2008.
- 372 Andreae, M. O., and Gelencser, A.: Black carbon or brown carbon? The nature of light-absorbing carbonaceous  
373 aerosols, *Atmos. Chem. Phys.*, 6, 3131-3148, <http://dx.doi.org/10.5194/acp-6-3131-2006>, 2006.
- 374 Atkinson, R.; Baulch, D. L.; Cox, R. A.; Crowley, J. N.; Hampson, R. F.; Hynes, R. G.; Jenkin, M. E.; Rossi, M. J.;  
375 Troe, J.: Evaluated kinetic and photochemical data for atmospheric chemistry: Volume II - gas phase reactions  
376 of organic species, *Atmos. Chem. Phys.*, 6, 3625-4055, <http://dx.doi.org/10.5194/acp-6-3625-2006>, 2006.
- 377 Birdwell, J. E., and Engel, A. S.: Characterization of dissolved organic matter in cave and spring waters using  
378 UV-Vis absorbance and fluorescence spectroscopy, *Org. Geochem.*, 41,  
379 <http://dx.doi.org/10.1016/j.orggeochem.2009.11.002>, 2010.
- 380 Budisulistiorini, S. H.; Riva, M.; Williams, M.; Chen, J.; Itoh, M.; Surratt, J. D.; Kuwata, M.: Light-Absorbing  
381 Brown Carbon Aerosol Constituents from Combustion of Indonesian Peat and Biomass. *Environ. Sci. Technol.*,  
382 51, 4415-4423, <http://dx.doi.org/10.1021/acs.est.7b00397>, 2017.
- 383 Canonica, S.; Hellrung, B.; Müller, P.; Wirz, J.: Aqueous Oxidation of Phenylurea Herbicides by Triplet Aromatic  
384 Ketones, *Environ. Sci. Technol.*, 40, 6636-6641, <https://doi.org/10.1021/es0611238>, 2006.
- 385 Carlton, A. G.; Turpin, B. J.; Altieri, K. E.; Seitzinger, S.; Reff, A.; Lim, H. J.; Ervens, B.: Atmospheric oxalic acid  
386 and SOA production from glyoxal: Results of aqueous photooxidation experiments, *Atmos. Environ.*, 41, 7588-  
387 7602, <http://dx.doi.org/10.1016/j.atmosenv.2007.05.035>, 2007.
- 388 Chen, Q., Miyazaki, Y., Kawamura, K., Matsumoto, K., Coburn, S., Volkamer, R., Iwamoto, Y., Kagami, S., Deng,  
389 Y., Ogawa, S., Ramasamy, S., Kato, S., Ida, A., Kajii, Y., and Mochida, M.: Characterization of Chromophoric  
390 Water-Soluble Organic Matter in Urban, Forest, and Marine Aerosols by HR-ToF-AMS Analysis and  
391 Excitation-Emission Matrix Spectroscopy, *Environ. Sci. Technol.*, 50, 10351-10360,  
392 <http://dx.doi.org/10.1021/acs.est.6b01643>, 2016a.
- 393 Chen, Q. C., Ikemori, F., and Mochida, M.: Light Absorption and Excitation-Emission Fluorescence of Urban  
394 Organic Aerosol Components and Their Relationship to Chemical Structure, *Environ. Sci. Technol.*, 50, 10859-  
395 10868, <http://dx.doi.org/10.1021/acs.est.6b02541>, 2016b.
- 396 Chen, Q., Li, J., Hua, X., Jiang, X., Mu, Z., Wang, M., Wang, J., Shan, M., Yang, X., Fan, X., Song, J., Wang, Y.,  
397 Guan, D., and Du, L.: Identification of species and sources of atmospheric chromophores by fluorescence  
398 excitation-emission matrix with parallel factor analysis, *Sci. Total Environ.*, 718, 137322,  
399 <http://dx.doi.org/10.1016/j.scitotenv.2020.137322>, 2020.
- 400 Chen, Q.; Mu, Z.; Xu, L.; Wang, M.; Wang, J.; Shan, M.; Fan, X.; Song, J.; Wang, Y.; Lin, P.; Du, L.: Triplet-state  
401 organic matter in atmospheric aerosols: Formation characteristics and potential effects on aerosol aging, *Atmos.*  
402 *Environ.*, 252, 118343, <https://doi.org/10.1016/j.atmosenv.2021.118343>, 2021.
- 403 Chen, Y., Zhang, X., and Feng, S.: Contribution of the Excited Triplet State of Humic Acid and Superoxide Radical  
404 Anion to Generation and Elimination of Phenoxyl Radical, *Environ. Sci. Technol.*, 52, 8283-8291,  
405 <http://dx.doi.org/10.1021/acs.est.8b00890>, 2018.
- 406 Cheng, Y., He, K. B., Du, Z. Y., Engling, G., Liu, J. M., Ma, Y. L., Zheng, M., and Weber, R. J.: The characteristics  
407 of brown carbon aerosol during winter in Beijing, *Atmos. Environ.*, 127, 355-364,  
408 <http://dx.doi.org/10.1016/j.atmosenv.2015.12.035>, 2016.
- 409 Claeys, M.; Graham, B.; Vas, G.; Wang, W.; Vermeylen, R.; Pashynska, V.; Cafmeyer, J.; Guyon, P.; Andreae, M.  
410 O.; Artaxo, P.; Maenhaut, W.: Formation of secondary organic aerosols through photooxidation of isoprene,  
411 *Science*, 303, 1173-1176, <http://dx.doi.org/10.1126/science.1092805>, 2004.
- 412 Coble, P. G.: Marine optical biogeochemistry: the chemistry of ocean color, *Chem. Rev.*, 107, 402-418,  
413 <http://dx.doi.org/10.1021/cr050350+>, 2007.
- 414 Duarte, R. M. B. O., Pio, C. A., and Duarte, A. C.: Spectroscopic study of the water-soluble organic matter isolated  
415 from atmospheric aerosols collected under different atmospheric conditions, *Anal. Chim. Acta*, 530, 7-14,  
416 <http://dx.doi.org/10.1016/j.aca.2004.08.049>, 2005.

417 Encinas, M. V.; Lissi, E. A.; Olea, A. F.: Quenching of triplet benzophenone by vitamins E and C and by sulfur  
418 containing amino acids and peptides, *Photochem. Photobiol.*, 42, 347-52, <http://dx.doi.org/10.1111/j.1751->  
419 1097.1985.tb01580.x, 1985.

420 Fellman, J. B., Miller, M. P., Cory, R. M., D'Amore, D. V., and White, D.: Characterizing Dissolved Organic Matter  
421 Using PARAFAC Modeling of Fluorescence Spectroscopy: A Comparison of Two Models, *Environ. Sci.*  
422 *Technol.*, 43, 6228-6234, <http://dx.doi.org/10.1021/es900143g>, 2009.

423 George, C.; Ammann, M.; D'Anna, B.; Donaldson, D. J.; Nizkorodov, S. A.: Heterogeneous Photochemistry in the  
424 Atmosphere. *Chem. Rev.*, 115, 4218-4258, 10.1021/cr500648z, 2015.

425 Gonsior, M., Peake, B. M., Cooper, W. T., Podgorski, D., D'Andrilli, J., and Cooper, W. J.: Photochemically induced  
426 changes in dissolved organic matter identified by ultrahigh resolution fourier transform ion cyclotron resonance  
427 mass spectrometry, *Environ. Sci. Technol.*, 43, 698-703, <http://dx.doi.org/10.1021/es8022804>, 2009.

428 Graber, E. R., and Rudich, Y.: Atmospheric HULIS: how humic-like are they? A comprehensive and critical review,  
429 *Atmos. Chem. Phys.*, 6, 729-753, <http://dx.doi.org/10.5194/acp-6-729-2006>, 2005.

430 Grieshop, A. P., Donahue, N. M., and Robinson, A. L.: Laboratory investigation of photochemical oxidation of  
431 organic aerosol from wood fires 2: analysis of aerosol mass spectrometer data, *Atmos. Chem. Phys.*, 9, 2227-  
432 2240, <http://dx.doi.org/DOI.10.5194/acp-9-2227-2009>, 2009.

433 Haag, W. R., and Gassman, E.: Singlet oxygen in surface waters-Part II: Quantum yields of its production by some  
434 natural humic materials as a function of wavelength, *Chemosphere*, 13, 641-650,  
435 [http://dx.doi.org/10.1016/0045-6535\(84\)90200-5](http://dx.doi.org/10.1016/0045-6535(84)90200-5), 1984.

436 Harrison, A.W., Waterson, A.M., De Bruyn, W.J.: Spectroscopic and Photochemical Properties of Secondary Brown  
437 Carbon from Aqueous Reactions of Methylglyoxal, *ACS Earth Space Chem.*, 4, 762-773,  
438 <http://dx.doi.org/10.1021/acsearthspacechem.0c00061>, 2020.

439 Haynes, J. P., Miller, K. E., and Majestic, B. J.: Investigation into Photoinduced Auto-Oxidation of Polycyclic  
440 Aromatic Hydrocarbons Resulting in Brown Carbon Production, *Environ. Sci. Technol.*, 53, 682-691,  
441 <http://dx.doi.org/10.1021/acs.est.8b05704>, 2019.

442 Holmes, B. J., and Petrucci, G. A.: Water-soluble oligomer formation from acid-catalyzed reactions of levoglucosan  
443 in proxies of atmospheric aqueous aerosols, *Environ. Sci. Technol.*, 40, 4983-4989,  
444 <http://dx.doi.org/10.1021/es060646c>, 2006.

445 Hugué, A., Vacher, L., Relexans, S., Saubusse, S., Froidefond, J. M., and Parlanti, E.: Properties of fluorescent  
446 dissolved organic matter in the Gironde Estuary, *Org. Geochem.*, 40,  
447 <http://dx.doi.org/10.1016/j.orggeochem.2009.03.002>, 2009.

448 Jo, D. S.; Park, R. J.; Lee, S.; Kim, S. W.; Zhang, X.: A global simulation of brown carbon: implications for  
449 photochemistry and direct radiative effect, *Atmos. Chem. Phys.*, 16, 3413-3432, [http://dx.doi.org/10.5194/acp-](http://dx.doi.org/10.5194/acp-16-3413-2016)  
450 16-3413-2016, 2016.

451 Karanasiou, A., Minguillón, M. C., Viana, M., Alastuey, A., Putaud, J.-P., Maenhaut, W., Panteliadis, P., Močnik,  
452 G., Favez, O., and Kuhlbusch, T. A. J.: Thermal-optical analysis for the measurement of elemental carbon (EC)  
453 and organic carbon (OC) in ambient air a literature review, *Atmos. Meas. Tech. Discuss.*, 8, 9649-9712,  
454 <http://dx.doi.org/10.5194/amtd-8-9649-2015>, 2015.

455 Kaur, R., and Anastasio, C.: First Measurements of Organic Triplet Excited States in Atmospheric Waters, *Environ.*  
456 *Sci. Technol.*, 52, 5218-5226, <http://dx.doi.org/10.1021/acs.est.7b06699>, 2018.

457 Latch, D. E., and McNeill, K.: Microheterogeneity of singlet oxygen distributions in irradiated humic acid solutions,  
458 *Science*, 311, 1743-1747, <http://dx.doi.org/10.1126/science.1121636>, 2006.

459 Lee, H. J., Laskin, A., Laskin, J., and Nizkorodov, S. A.: Excitation-emission spectra and fluorescence quantum  
460 yields for fresh and aged biogenic secondary organic aerosols, *Environ. Sci. Technol.*, 47, 5763-5770,  
461 <http://dx.doi.org/10.1021/es400644c>, 2013.

462 Lee, H. J., Aiona, P. K., Laskin, A., Laskin, J., and Nizkorodov, S. A.: Effect of solar radiation on the optical  
463 properties and molecular composition of laboratory proxies of atmospheric brown carbon, *Environ. Sci.*  
464 *Technol.*, 48, 10217-10226, <http://dx.doi.org/10.1021/es502515r>, 2014.

465 Liu, J. M., Lin, P., Laskin, A., Laskin, J., Kathmann, S. M., Wise, M., Caylor, R., Imholt, F., Selimovic, V., and  
466 Shilling, J. E.: Optical properties and aging of light-absorbing secondary organic aerosol, *Atmos. Chem. Phys.*,  
467 16, 12815-12827, <http://dx.doi.org/10.5194/acp-16-12815-2016>, 2016.

468 Maizel, A. C., Li, J., and Remucal, C. K.: Relationships Between Dissolved Organic Matter Composition and  
469 Photochemistry in Lakes of Diverse Trophic Status, *Environ. Sci. Technol.*, 51, 9624-9632,  
470 <http://dx.doi.org/10.1021/acs.est.7b01270>, 2017.

471 Mang, S. A.; Henricksen, D. K.; Bateman, A. P.; Andersen, M. P. S.; Blake, D. R.; Nizkorodov, S. A.: Contribution  
472 of Carbonyl Photochemistry to Aging of Atmospheric Secondary Organic Aerosol, *J. Phys. Chem. A*, 112,  
473 8337-8344, <http://dx.doi.org/10.1021/jp804376c>, 2008.

474 Marciniak, B.; Bobrowski, K.; Hug, G. L.: Quenching of triplet states of aromatic ketones by sulfur-containing  
475 amino acids in solution. Evidence for electron transfer, *J. Phys. Chem.*, 97, 11937-11943, 10.1021/j100148a015,  
476 1993.

477 McKnight, D. M., Boyer, E. W., Westerhoff, P. K., Doran, P. T., Kulbe, T., and Andersen, D. T.: Spectrofluorometric  
478 characterization of dissolved organic matter for indication of precursor organic material and aromaticity,  
479 *Limnol. Oceanogr.*, 46, 38-48, <http://dx.doi.org/10.4319/lo.2001.46.1.0038>, 2001.

480 McNeill, K., and Canonica, S.: Triplet state dissolved organic matter in aquatic photochemistry: reaction  
481 mechanisms, substrate scope, and photophysical properties, *Environ. Sci. Process Impacts*, 18, 1381-1399,  
482 <http://dx.doi.org/10.1039/c6em00408c>, 2016.

483 Moor, K. J., Schmitt, M., Erickson, P. R., and McNeill, K.: Sorbic Acid as a Triplet Probe: Triplet Energy and  
484 Reactivity with Triplet-State Dissolved Organic Matter via  $^{1}O_2$  Phosphorescence, *Environ. Sci. Technol.*,  
485 <http://dx.doi.org/10.1021/acs.est.9b01787>, 2019.

486 Mu, Z., Chen, Q. C., Wang, Y. Q., Shen, Z. X., Hua, X. Y., Zhang, Z. M., Sun, H. Y., Wang, M. M., and Zhang, L.  
487 X.: Characteristics of Carbonaceous Aerosol Pollution in PM<sub>2.5</sub> in Xi'an, *Huan Jing Ke Xue*, 40, 1529-1536,  
488 <http://dx.doi.org/10.13227/j.hjkk.201807135>, 2019.

489 Murphy, K. R., Stedmon, C. A., Graeber, D., and Bro, R.: Fluorescence spectroscopy and multi-way techniques.  
490 PARAFAC, *Anal. Methods*, 5, 6557-6566, <http://dx.doi.org/10.1039/c3ay41160e>, 2013.

491 Nebbioso, A.; Piccolo, A.: Molecular characterization of dissolved organic matter (DOM): a critical review, *Anal.*  
492 *Bioanal., Chem.* 405, 109-124, <http://dx.doi.org/10.1007/s00216-012-6363-2>, 2013.

493 Paul Hansard, S., Vermilyea, A. W., and Voelker, B. M.: Measurements of superoxide radical concentration and  
494 decay kinetics in the Gulf of Alaska, *Deep Sea Res., Part I*, 57, 1111-1119,  
495 <http://dx.doi.org/10.1016/j.dsr.2010.05.007>, 2010.

496 Perri, M. J., Seitzinger, S., and Turpin, B. J.: Secondary organic aerosol production from aqueous photooxidation of  
497 glycolaldehyde: Laboratory experiments, *Atmos. Environ.*, 43, 1487-1497,  
498 <http://dx.doi.org/10.1016/j.atmosenv.2008.11.037>, 2009.

499 Richards-Henderson, N. K., Pham, A. T., Kirk, B. B., and Anastasio, C.: Secondary organic aerosol from aqueous  
500 reactions of green leaf volatiles with organic triplet excited states and singlet molecular oxygen, *Environ. Sci.*  
501 *Technol.*, 49, 268-276, <http://dx.doi.org/10.1021/es503656m>, 2015.

502 Rosado-Lausell, S.L., Wang, H.T., Gutierrez, L., Romero-Maraccini, O.C., Niu, X.Z., Gin, K.Y.H., Croue, J.P.,  
503 Nguyen, T.H.: Roles of singlet oxygen and triplet excited state of dissolved organic matter formed by different  
504 organic in bacteriophage MS2 inactivation, *Water Res.*, 47, 4869-4879,  
505 <http://dx.doi.org/10.1016/j.watres.2013.05.018>, 2013.

506 Rosario-Ortiz, F. L., and Canonica, S.: Probe Compounds to Assess the Photochemical Activity of Dissolved  
507 Organic Matter, *Environ. Sci. Technol.*, 50, 12532-12547, <http://dx.doi.org/10.1021/acs.est.6b02776>, 2016.

508 Saleh, R., Hennigan, C. J., McMeeking, G. R., Chuang, W. K., Robinson, E. S., Coe, H., Donahue, N. M., and  
509 Robinson, A. L.: Absorptivity of brown carbon in fresh and photo-chemically aged biomass-burning emissions,  
510 *Atmos. Chem. Phys.*, 13, 7683-7693, <http://dx.doi.org/10.5194/acp-13-7683-2013>, 2013.

511 Sharpless, C. M.: Lifetimes of Triplet Dissolved Natural Organic Matter (DOM) and the Effect of NaBH<sub>4</sub> Reduction  
512 on Singlet Oxygen Quantum Yields: Implications for DOM Photophysics, *Environ. Sci. Technol.*, 46, 4466-  
513 4473, <http://dx.doi.org/10.1021/es300217h>, 2012.

514 Sierra, M. M. D., Giovanela, M., Parlanti, E., and Soriano-Sierra, E. J.: Fluorescence fingerprint of fulvic and humic  
515 acids from varied origins as viewed by single-scan and excitation/emission matrix techniques, *Chemosphere*,  
516 58, <http://dx.doi.org/10.1016/j.chemosphere.2004.09.038>, 2005.

517 Stewart, A. J.; Wetzel, R. G.: Fluorescence: absorbance ratios—a molecular-weight tracer of dissolved organic matter,  
518 *Limnol. Oceanogr.*, 25, 559-564, <https://doi.org/10.4319/lo.1980.25.3.0559>, 1980.

519 Szymczak, R., and Waite, T.: Generation and decay of hydrogen peroxide in estuarine waters, *Mar. Freshwater Res.*,  
520 39, 289-299, <http://dx.doi.org/10.1071/MF9880289>, 1988.

521 Tang, J., Li, J., Su, T., Han, Y., Mo, Y.Z., Jiang, H.X., Cui, M., Jiang, B., Chen, Y.J., Tang, J.H., Song, J.Z., Peng,  
522 P.A., Zhang, G.: Molecular compositions and optical properties of dissolved brown carbon in biomass burning,  
523 coal combustion, and vehicle emission aerosols illuminated by excitation-emission matrix spectroscopy and  
524 Fourier transform ion cyclotron resonance mass spectrometry analysis. *Atmos. Chem. Phys.* 20, 2513-2532,  
525 <http://dx.doi.org/10.5194/acp-20-2513-2020>, 2020a.

526 Tang, S. S., Li, F. H., Tsona, N. T., Lu, C. Y., Wang, X. F., and Du, L.: Aqueous-Phase Photooxidation of Vanillic  
527 Acid: A Potential Source of Humic-Like Substances (HULIS), *Acs Earth and Space Chem.*, 4, 862-872,  
528 <http://dx.doi.org/10.1021/acsearthspacechem.0c00070>, 2020b.

529 Timko, S.; Maydanov, A.; Pittelli, S.; Conte, M.; Cooper, W.; Koch, B.; Schmitt-Kopplin, P.; Gonsior, M.: Depth-  
530 dependent photodegradation of marine dissolved organic matter, *Front. Mar. Sci.*, 2,  
531 <https://doi.org/10.3389/fmars.2015.00066>, 2015.

532 Tranvik, L.; Kokalj, S.: Decreased biodegradability of algal DOC due to interactive effects of UV radiation and  
533 humic matter, *Aquat. Microb. Ecol.*, 14, 301-307, <https://doi.org/10.3354/ame014301>, 1998.

534 Wawzonek, S.; Laitinen, H. A.: The Reduction of Unsaturated Hydrocarbons at the Dropping Mercury Electrode.  
535 II. Aromatic Polynuclear Hydrocarbons, *J. Am. Chem. Soc.*, 64, 2365-2368,  
536 <http://dx.doi.org/10.1021/ja01262a040>, 1942.

537 Wenk, J., Aeschbacher, M., Salhi, E., Canonica, S., von Gunten, U., and Sander, M.: Chemical oxidation of dissolved  
538 organic matter by chlorine dioxide, chlorine, and ozone: effects on its optical and antioxidant properties,  
539 *Environ. Sci. Technol.*, 47, 11147-11156, <http://dx.doi.org/10.1021/es402516b>, 2013.

540 Wong, J. P. S., Zhou, S. M., and Abbatt, J. P. D.: Changes in Secondary Organic Aerosol Composition and Mass  
541 due to Photolysis: Relative Humidity Dependence, *J. Phys. Chem. A*, 119, 4309-4316,  
542 <http://dx.doi.org/10.1021/jp506898c>, 2015.

543 Xu, W.; Gao, Q.; He, C.; Shi, Q.; Hou, Z.-Q.; Zhao, H.-Z.: Using ESI FT-ICR MS to Characterize Dissolved Organic  
544 Matter in Salt Lakes with Different Salinity, *Environ. Sci. Technol.*, 54, 12929-12937,  
545 <http://dx.doi.org/10.1021/acs.est.0c01681>, 2020.

546 Yang, X. M.; Yuan, J.; Yue, F. J.; Li, S. L.; Wang, B. L.; Mohinuzzaman, M.; Liu, Y. J.; Senesi, N.; Lao, X. Y.; Li,  
547 L. L.; Liu, C. Q.; Ellam, R. M.; Vione, D.; Mostofa, K. M. G.: New insights into mechanisms of sunlight- and  
548 dark-mediated high-temperature accelerated diurnal production-degradation of fluorescent DOM in lake waters,  
549 *Sci. Total Environ.*, 760, 14, <http://dx.doi.org/10.1016/j.scitotenv.2020.143377>, 2021.



550 Zappoli, S., Andracchio, A., Fuzzi, S., Facchini, M. C., Gelencser, A., Kiss, G., Krivacsy, Z., Molnar, A., Meszaros,  
551 E., Hansson, H. C., Rosman, K., and Zebuhr, Y.: Inorganic, organic and macromolecular components of fine  
552 aerosol in different areas of Europe in relation to their water solubility, *Atmos. Environ.*, 33, 2733-2743,  
553 [http://dx.doi.org/10.1016/S1352-2310\(98\)00362-8](http://dx.doi.org/10.1016/S1352-2310(98)00362-8), 1999.

554 Zepp, R. G., Schlotzhauer, P. F., and Sink, R. M.: Photosensitized transformations involving electronic energy  
555 transfer in natural waters: role of humic substances, *Environ. Sci. Technol.*, 19, 74-81,  
556 <http://dx.doi.org/10.1021/es00131a008>, 1985.

557 Zhang, D., Yan, S., and Song, W.: Photochemically induced formation of reactive oxygen species (ROS) from  
558 effluent organic matter, *Environ. Sci. Technol.*, 48, 12645-12653, <http://dx.doi.org/10.1021/es5028663>, 2014.

559 Zhao, R., Lee, A. K. Y., Huang, L., Li, X., Yang, F., and Abbatt, J. P. D.: Photochemical processing of aqueous  
560 atmospheric brown carbon, *Atmos. Chem. Phys.*, 15, 6087-6100, <http://dx.doi.org/10.5194/acp-15-6087-2015>,  
561 2015.

562 Zhao, Y.; Hallar, A. G.; Mazzoleni, L. R: Atmospheric organic matter in clouds: exact masses and molecular formula  
563 identification using ultrahigh-resolution FT-ICR mass spectrometry, *Atmos. Chem. Phys.*, 13, 12343-12362,  
564 <http://dx.doi.org/10.5194/acp-13-12343-2013>, 2013.

565 Zhong, M., and Jang, M.: Dynamic light absorption of biomass-burning organic carbon photochemically aged under  
566 natural sunlight, *Atmos. Chem. Phys.*, 14, 1517-1525, <http://dx.doi.org/10.5194/acp-14-1517-2014>, 2014.

567 Zhou, H., Yan, S., Lian, L., and Song, W.: Triplet-State Photochemistry of Dissolved Organic Matter: Triplet-State  
568 Energy Distribution and Surface Electric Charge Conditions, *Environ. Sci. Technol.*, 53, 2482-2490,  
569 <http://dx.doi.org/10.1021/acs.est.8b06574>, 2019.